Interference effects on the critical current in a clean-limit superconductor—normal-metal—superconductor junction

Hideaki Takayanagi, Tatsushi Akazaki, and Junsaku Nitta

NTT Basic Research Laboratories, 3-1, Morinosato-Wakamiya, Atsugi-shi, Kanagawa 243-01, Japan
(Received 5 October 1994)

Interference effects are confirmed on the critical current of a gate-fitted superconductor—normal-metal—superconductor junction in the clean limit. As the normal metal, the junction uses a two-dimensional electron gas (2DEG) with a high mobility of 7.38 m^2/V s and a high carrier density of 1.98×10^{12} cm^{-2} at 4.2 K. The superconducting critical current that flows through the 2DEG is measured as a function of the gate voltage and shows oscillations as a function of the 2DEG carrier concentration. This oscillation is explained by the interference effects predicted by Chrestin et al. The typical period of the oscillation agrees well with the theoretical prediction.

It is well-known that at the interface of a normal metal (N) and a superconductor (S) there occurs Andreev reflection, i.e., an incident electron (hole) from the normal side is reflected as a hole (electron).[1] The quantum transport of an S-N junction shows various interesting effects due to Andreev reflection, e.g., modifications of weak localization and universal conductance fluctuations[2] or a quasiparticle interferometer.[3] Recently a second-quantization description of Andreev reflection was given.[4] In an S-N-S junction, it is theoretically shown that supercurrent is carried mainly through the bound states generated by Andreev reflection. For the superconducting transport in a dirty-limit S-N-S junction, interference effects[5] and interaction effects associated with Anderson localization[6] have been studied and both were experimentally confirmed by the authors.[7,8] In a clean-limit S-N-S junction, a superconducting quantum point contact (SQPC) was proposed.[9,10] In attempts to achieve SQPC S-N-S junctions, the use of a two-dimensional electron gas (2DEG) in the clean limit have been studied.[11–14]

Chrestin et al. calculated the critical current I_c in a clean-limit S-2DEG-S junction and found that it oscillates with the carrier concentration of the 2DEG.[15] They stated this oscillation was due to the interference of the quasiparticles that undergo two normal reflections between two Andreev reflections [Fig. 1(c)]. In this paper, we report an experimental confirmation of the I_c oscillations due to the interference effect in a gate-fitted $In_{0.52}Al_{0.48}As/In_{0.53}Ga_{0.47}As$ heterostructure-coupled S-N-S junction and we compare the experimental results with the theoretical predictions.

Figure 1(a) is a schematic of the fabricated junction coupled with an InAs-inserted-channel $In_{0.52}Al_{0.48}As/In_{0.53}Ga_{0.47}As$ heterostructure. The heterostructure was grown by molecular-beam epitaxy (MBE) on Fe-doped semi-insulating InP substrate. The fabrication process for the junction is as follows. First, the 60-nm undoped InAlAs layer was chemically etched, then the 11-nm undoped InGaAs layer was removed by Ar rf sputter cleaning. Two 100-nm-thick Nb electrodes were then deposited on the InAs layer by electron-beam deposition. Next, the 0.1-μm-thick SiO_2 gate-insulator film was deposited. Finally, the Al gate metal was deposited. The details of the fabrication process for the junction are

discussed elsewhere.[16] The 2DEG is confined in the inserted 4-nm InAs layer and has a high mobility and a high carrier concentration.[17] Two superconducting Nb electrodes are coupled with the 2DEG. The separation between the two Nb electrodes L was in the 0.2 to 0.6 μm range. In this range, it was experimentally confirmed that the supercurrent flowed through the 2DEG up to about 6.5 K. The gate struc-
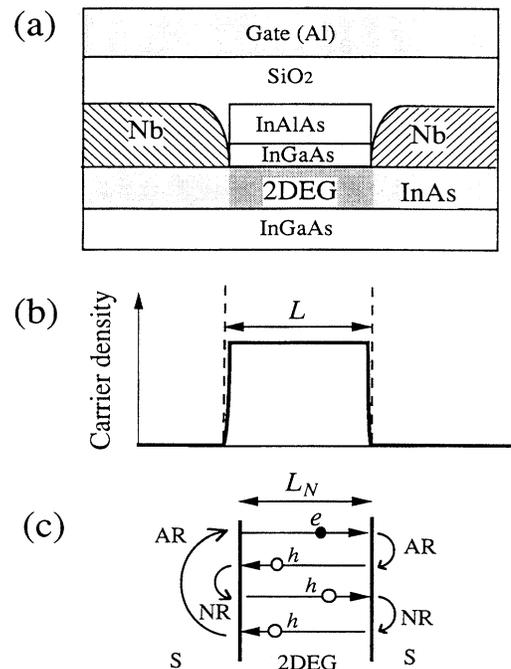

FIG. 1. (a) Cross-sectional view of the fabricated junction. The supercurrent flows through the two-dimensional gas formed in the inserted InAs layer into the heterostructure and is changed by the gate voltage. (b) Schematic view of the carrier density distribution. The carrier concentration in the InAs layer underneath the Nb electrodes is strongly suppressed. (c) The lowest-order process, which involves two Andreev (AR) and two normal (NR) reflections, contributed to the oscillation of the critical current.
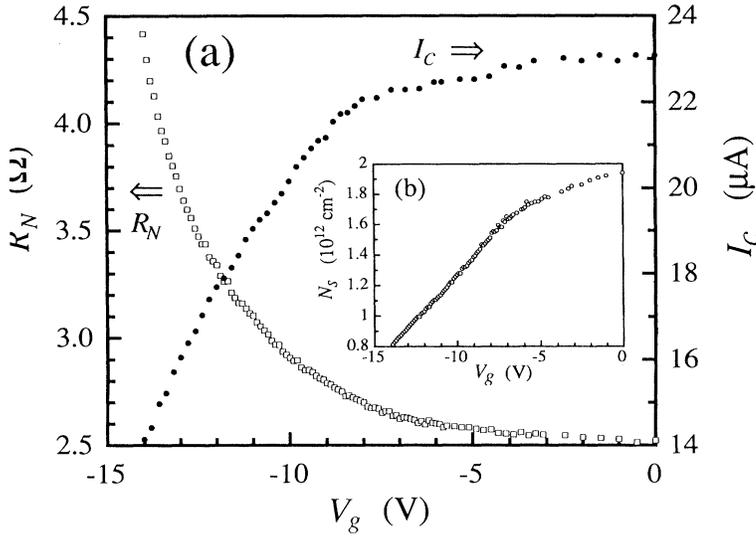
FIG. 2. (a) Measured critical current I_c and the junction normal resistance R_N for the junction with $L = 0.4$ μm and $W = 80$ μm as a function of the gate voltage V_g at 0.74 K. I_c shows clear oscillations. (b) Carrier concentration N_s of the 2DEG as a function of V_g. This curve is obtained from R_N-V_g curve and the relations in Eq. (1).

ture could reproducibly withstand a gate voltage V_g of up to -20 V applied to the gate. This gate configuration made it possible to vary the carrier concentration and mobility of the 2DEG by the gate voltage and this resulted in changes in both the superconducting critical current I_c and the normal resistance R_N of the junction. This property is the main feature of this three-terminal device (Josephson field-effect transistor).[18]

The carrier concentration, N_s, the mobility, μ, and the effective mass, m^*, of the 2DEG used in this study were respectively determined to be 1.98×10^{12} cm^{-2}, 73 800 cm^2/V s, and $0.05m_e$, at 4.2 K by Shubnikov-de Haas (SdH) measurement. Here, m_e is the free electron mass. From these values, the coherence length $\xi_N = \hbar v_F/2\pi k_B T$ in the clean limit and the mean free path, l, were calculated to be 0.23 μm at 4.2 K and 1.7 μm, respectively, where v_F is the Fermi velocity. Therefore, the junction belongs to the clean limit ($l > \xi_N$) with ballistic transport ($l \gg L$) when $V_g = 0$. There are some reports of gate-voltage operation of an S-N-S junction in the dirty limit.[19] However, this is, to our knowledge, the first report of such operation in the clean limit. By definition, ξ_N increases as temperature decreases and at a low temperature ξ_N does not satisfy the clean limit condition ($l > \xi_N$) since l does not show a strong temperature dependence below 4.2 K. However, it is noteworthy that ξ_N is no longer a useful length scale when $L < \xi_N$.[15] The system can be considered to be the clean limit also in this case.

When a large gate voltage is applied, the situation is different. Because both N_s and μ decrease as the absolute value of the gate voltage increases, $l = \hbar\mu(2\pi N_s)^{1/2}/e$ decreases more rapidly than ξ_N. The crossover from the clean limit to the dirty limit $[l < \xi_N = (\hbar^3 \mu N_s/2k_B Tem^*)^{1/2}]$ was observed for a junction with $L = 0.4$ μm.[16] However, ballistic transport ($l > L$) was still kept in the carrier concentration regime ($2 \times 10^{12} > N_s > 0.8 \times 10^{12}$ cm^{-2}) studied in this paper.

When the two top layers, InAlAs and InGaAs, were etched gradually, N_s of the 2DEG confined in the InAs layer decreased since the band edge of the InAs layer was pulled up to a higher energy position.[20] When the two top layers were finally removed, the 2DEG disappeared. The inserted

InAs layer was originally undoped. Therefore, the carrier concentration in the InAs layer underneath the Nb electrodes became very low, as shown in Fig. 1(b). As discussed in Ref. 15, the oscillation of I_c requires a rigid boundary condition at the 2DEG-S interface. The 2DEG structure discussed here may satisfy this boundary condition and may result in the I_c oscillation. The InAs layer with a low carrier concentration between the 2DEG and the Nb electrode also explains the contact resistance R_{NC} discussed later.

Figure 2(a) shows the measured I_c and R_N for a junction as a function of the gate voltage V_g at $T = 0.74$ K. The coupling length L and the width W for the junction are 0.4 and 80 μm, respectively. The I_c of this type of junction structure is very sensitive to a magnetic field and there was a residual field around the junction. A small applied magnetic field was needed to suppress the residual field. For each gate voltage the maximum value of I_c was therefore found by carefully optimizing I_c with the help of a small magnetic field (about
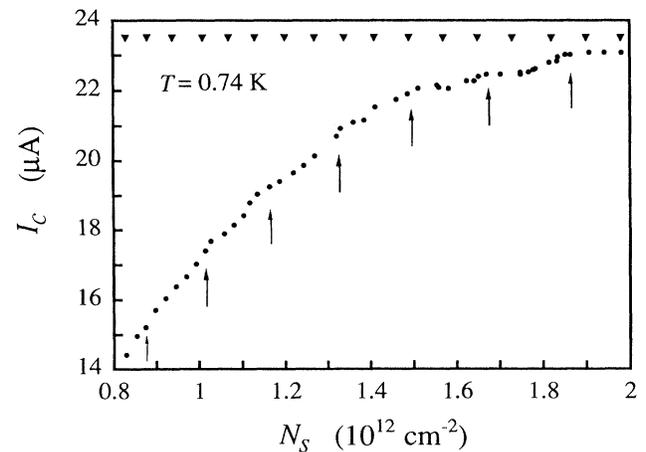

FIG. 3. Critical current as a function of the carrier concentration at 0.74 K. Small triangles in the figure denote the calculated peak positions for $L = L_N = 0.4$ μm. Arrows also denote ones for $L_N = 0.18$ μm.
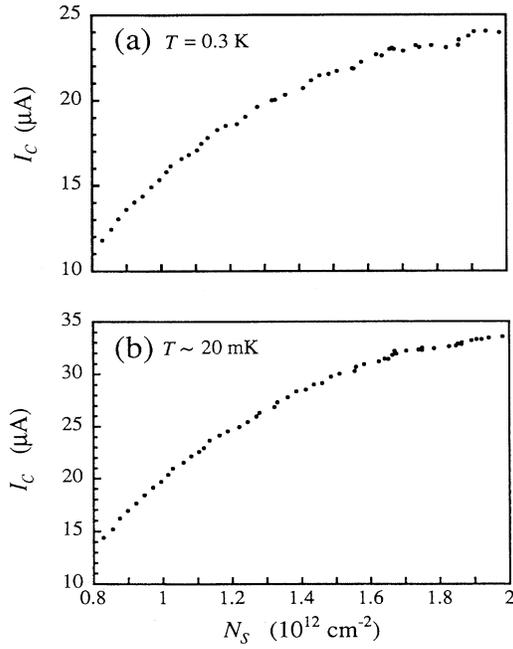
FIG. 4. Critical current as a function of the carrier concentration (a) at 0.3 K and (b) at about 20 mK. At both temperatures I_c oscillations can be seen.

0.1 G) applied perpendicular to the 2DEG. Over the range from 0 to -15 V, shown in Fig. 2(a), the magnitude of the applied magnetic field which maximized I_c was constant. R_N was determined as the differential resistance at a higher bias voltage than $2\Delta/e$, where Δ is the energy gap of Nb. The energy gap of bulk Nb is 1.5 meV, but we adopted 1 meV for the Nb electrode at the interface in our junction, as shown in Fig. 5.

From the R_N-V_g data and the relations

$$R_N = 2R_{NC} + R_{NS},$$

$$R_{NS} = L/eWN_s\mu,$$

$$\mu \propto N_s, \tag{1}$$

N_s as a function of V_g in Fig. 2(b) was obtained, where R_{NC} is the contact resistance at the S-2DEG interface and R_{NS} is the semiconductor channel (i.e., 2DEG) resistance. As discussed above, R_{NC} originates in the InAs layer with a low carrier concentration between the 2DEG and the Nb. Another origin for R_{NC} is the wave-number discrepancy between the superconductor and the 2DEG, which causes normal reflection.[3] R_{NC} is assumed to be constant at 1.13 Ω, which is calculated from the relations shown in Eq. (1) and N_s of 1.98×10^{12} cm^{-2}, μ of 73 800 cm^2/V s for the 2DEG at 4.2 K and $V_g = 0$. We determined μ and N_s for the 2DEG by SdH measurement with changing N_s and confirmed that μ depends on N_s in the relation $\mu \propto N_s^\gamma$ where γ is 1.[21]

In general, the $I_c R_N$ product of a superconducting weak link is almost constant when the change in I_c or R_N is small. Therefore, if R_N oscillates with a period of V_g, I_c oscillates with the same period. I_c shows clear oscillation as a function
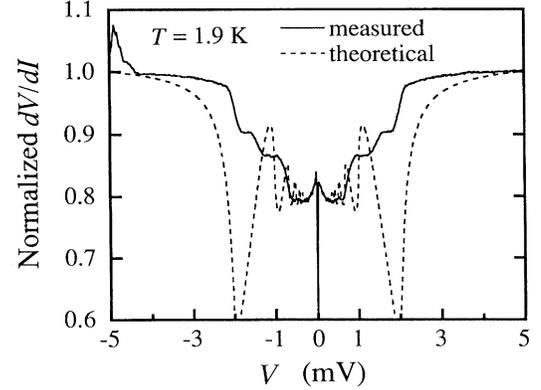

FIG. 5. Differential resistance as a function of voltage at 1.9 K. The dashed line represents the calculated plot for $\Delta_{NB} = 1.0$ meV and $Z = 0.65$. The calculation method is the same as that in Ref. 12.

of V_g as shown in Fig. 2(a). On the other hand, R_N or N_s does not show such oscillations. This fact indicates the I_c oscillation is not due to the change in R_N.

We will now discuss the experimental results of the I_c oscillations as a function of N_s. The data in Figs. 2(a) and 2(b) lead to the I_c-N_s characteristics as shown in Fig. 3. Figures 4(a) and 4(b) are also the N_s dependencies of I_c, which were obtained in the same way but the measurement temperatures were different [Fig. 4(a) for 0.3 K and 4(b) for about 20 mK]. Clear oscillations of I_c can be seen for every temperature and the peak positions of I_c for each temperature are almost the same as those for other temperatures. This indicates that the best explanation for these reproducible I_c oscillations is the interference of quasiparticles that undergo Andreev as well as normal reflections.[15]

First we discuss the period of the oscillations. According to calculations, the local peaks of I_c as a function of N_s are well approximated by

$$N_{s,\text{max}} = \frac{\pi}{2L_N^2} N^2. \tag{2}$$

The integer N is half the number of the quasiparticle states with "resonant" values of k_y, defined by the maxima of $\cos[2(k_F^2 - k_y^2)^{1/2}L_N]$, where k_F is the Fermi wave number given by $(2\pi N_s)^{1/2}$ and k_y is the wave number of the y direction, which is perpendicular to the current direction x. L_N is the distance the electron (hole) moves between the first normal reflection and the second one [Fig. 1(c)]. When a peak of I_c has N, the next smaller one has $N-1$ and the next larger one has $N+1$. First we calculated the peak positions of I_c for $L_N = 0.4$ μm. The calculated results did not agree with the experimental ones. In Fig. 3 the calculated peak positions for $L_N = 0.4$ μm are shown by small triangles. Then we calculated peak positions by changing L_N. The best fitting to the experimental data was obtained for $L_N = 0.18$ μm. The arrows in Fig. 3 show the calculated positions for $L_N = 0.18$ μm. This good agreement shows the I_c oscillation as a function of N_s obtained in this study is due to the interference effects predicted by Chrestin et al. It is not so clear why the calculated L_N is shorter than the actual $L = 0.4$

μm. It is probably due to the fact that real length of the 2DEG in the structure shown in Fig. (a)1 is shorter than L and L_N also becomes shorter than L.

Next we discuss the amplitude of the oscillation ΔI_c. According to the calculation, ΔI_c becomes larger with increasing N_s when the barrier strength at the interface (Ref. 22) Z, is not zero. The calculation also shows that ΔI_c increases when temperature decreases. For every temperature, ΔI_c showed an increase with increasing N_s as shown in Figs. 3 and 4. This is because $Z = 0.65$ for the measured junction as discussed later. The temperature dependence of ΔI_c seen in Figs. 3 and 4 is not so clear, since even $T = 0.74$ K is low enough to give a long ξ_N compared with L_N. The theory shows that ΔI_c decays asymptotically as $\exp(-2L_N/\xi_N)$. This means that ΔI_c has a temperature dependence of $\exp[-2L_N/\xi_N(T)]$. ΔI_c for the first peak in Figs. 3 and 4 are ~ 0.7 μA for 0.74 K, ~ 0.9 μA for 0.3 K, and ~ 1.0 μA for 20 mK. These values give a ratio of 1:1.3:1.4, which agrees with the calculated ratio of 1:1.2:1.3 obtained from $\exp[-2L_N/\xi_N(T)]$ and $L_N = 0.18$ μm.

The ratio, $\Delta I_c/I_c$, in Figs. 3 and 4 is very small compared with the theoretical results. The calculation for I_c-N_s was carried out for the rigid boundary condition (i.e., L is fixed). On the other hand, the actual L for the measured junction fluctuates spacially and so does L_N. It is considered that ΔI_c is suppressed because of the L_N fluctuations. However, if L_N fluctuates specially with a fine period in the y direction and with a scale like λ_F in the x direction, ΔI_c is strongly suppressed. Here, λ_F is the Fermi wavelength (e.g.,

$\lambda_F = 18$ nm at $N_s = 2 \times 10^{12}$ cm^{-2}). L_N probably changes smoothly in the x and y direction, resulting in measurable ΔI_c. There is another reason that the I_c oscillation could be observed in our junction. The theory shows the oscillation becomes more pronounced with increasing Z since the normal reflection increases and Andreev reflection decreases with increasing Z, where Z is the barrier strength[22] at the S-2DEG interface. As shown in Fig. 5, we measured dV/dI-V characteristics for the junction and obtained $Z = 0.65$ by comparing with the calculation taking into account of multiple Andreev reflections. This Z value reduces the amplitude of I_c but makes the amplitude of the I_c oscillations more pronounced.

In summary, the critical current for a superconductor–2DEG–superconductor in the clean limit was measured. The critical current showed oscillations as a function of the carrier concentration of the 2DEG. This result is the clear evidence that the oscillation is due to the interference effects of the quasiparticles that undergo Andreev as well as normal reflections. It is shown that the interference effects play an important role in the superconducting transport of an S-N-S junction not only in the dirty limit but also in the clean limit.

[1] A. F. Andreev, Zh. Eksp. Teor. Fiz. **46**, 1823 (1964) [Sov. Phys. JETP **19**, 1228 (1964)].

[2] See, e.g., C. W. J. Beenakker, in *Mesoscopic Physics*, edited by E. Akkermans, G. Montambaux, and J.-L. Pichard (North-Holland, Amsterdam, 1994).

[3] H. Nakano and H. Takayanagi, Solid State Commun. **80**, 997 (1991); Phys. Rev. B **47**, 7986 (1993).

[4] H. Nakano and H. Takayanagi, Phys. Rev. B **50**, 3139 (1994).

[5] B. L. Al'tshuler and B. Z. Spivak, Zh. Eksp. Teor. Fiz. **92**, 609 (1987) [Sov. Phys. JETP **65**, 343 (1987)].

[6] H. Fukuyama and S. Maekawa, J. Phys. Soc. Jpn. **55**, 1814 (1986).

[7] H. Takayanagi, Jørn B. Hansen, and J. Nitta, in *Mesoscopic Superconductivity*, Nato Advanced Research Workshop (Karlsruhe, 1994), edited by G. Schön and D. Averin [Physica B (to be published)]; Phys. Rev. Lett. (to be published).

[8] H. Takayanagi, Jørn B. Hansen, and J. Nitta, Phys. Rev. Lett. (to be published).

[9] C. W. J. Beenakker and H. van Houten, Phys. Rev. Lett. **66**, 3056 (1991).

[10] A. Furusaki, H. Takayanagi, and M. Tsukada, Phys. Rev. Lett. **67**, 132 (1991); Phys. Rev. B **45**, 10 563 (1992).

[11] C. Nguyen, J. Werking, H. Kroemer, and E. L. Hu, Appl. Phys. Lett. **57**, 87 (1992).

[12] J. Nitta, T. Akazaki, H. Takayanagi, and K. Arai, Phys. Rev. B **46**, 14 286 (1992); **49**, 3659 (1994).

[13] K.-M. H. Lenssen, M. Matters, C. J. P. M. Harmans, J. E. Mooij, M. R. Leys, W. van der Vleuten, and J. H. Wolter, IEEE Trans. Appl. Supercond. **3**, 1961 (1993).

[14] J. Nitta, T. Akazaki, and H. Takayanagi, Phys. Rev. B **49**, 3659 (1994).

[15] A. Chrestin, T. Matsuyama, and U. Merkt, Phys. Rev. B **49**, 498 (1994).

[16] H. Takayanagi, T. Akazaki, J. Nitta, and T. Enoki, Jpn. J. Appl. Phys. (to be published).

[17] T. Akazaki, J. Nitta, H. Takayanagi, T. Enoki, and K. Arai, Appl. Phys. Lett. **65**, 1263 (1994).

[18] A. W. Kleinsasser and W. J. Gallagher, in *Superconducting Devices*, edited by S. T. Ruggiero and D. A. Rudman (Academic, San Diego, 1990).

[19] H. Takayanagi and T. Kawakami, Phys. Rev. Lett. **54**, 2449 (1985), and references in Ref. 18.

[20] N. van der Post, J. Nitta, and H. Takayanagi, Appl. Phys. Lett. **63**, 2555 (1993).

[21] T. Akazaki and H. Takayanagi (unpublished).

[22] G. E. Blonder, M. Tinkham, and T. M. Klapwijk, Phys. Rev. B **25**, 4515 (1982).